The Mars Phoenix Communications Brownout during Entry into the Martian Atmosphere

David Morabito,* Richard Kornfeld,† Kristoffer Bruvold,‡ Lynn Craig,▲ and Karl Edquist△

Propagation of radio signals through sufficiently dense plasma will become disrupted during a space vehicle's hypersonic entry phase into a planetary atmosphere. The Mars Phoenix communication links were found to experience varying levels of reduced received signal strength (brownout) during the spacecraft's entry into the Martian atmosphere on May 25, 2008. These fades were attributed to charged particles generated inside the entry vehicle's high-temperature shock layer during the hypersonic entry. This article presents the results of the analysis of the UHF carrier signal power emitted by Phoenix as received by three orbiting relay satellites during the period around peak heating: Mars Reconnaissance Orbiter, Mars Odyssey, and Mars Express.

I. Introduction

During planetary atmospheric entry at hypersonic velocities, a spacecraft will be enveloped by a sheath of ionized particles as a result of the dissociation and subsequent ionization of the atmospheric gases (97 percent CO_2 and 3 percent N_2 by mass in the freestream) as they are heated and compressed by the shock or heated within the adjacent boundary layer. When the electron number density traversing the signal path gets sufficiently high, exceeding the critical value for a particular link frequency, communications can become disrupted. The degradation takes the form of added attenuation or even blackout, caused by reflection or absorption of signal energy at the link frequency. There are other factors that can cause signal degradation through the plasma sheath about the vehicle during atmospheric entry. These include distortion due to refraction (ray bending due to the plasma density irregularities) as the transmitted signal propagates through the shock layer as well as potential increased receiver noise temperature affecting the signal-to-noise ratio (SNR) based on heating through the aeroshell due to the high temperature of the plasma [1].

The Phoenix Mars Lander was launched on August 4, 2007, and landed in the plains of the northern polar region of Mars on May 25, 2008. A sophisticated strategy was employed for

* Communication Architectures and Research Section.
† Systems Engineering Section.
‡ Flight Communications Systems Section.
▲ Mission Design and Navigation Section; now with NASA Johnson Space Center, Houston, Texas.
△ NASA Langley Research Center, Hampton, Virginia.

The research described in this publication was carried out by the Jet Propulsion Laboratory, California Institute of Technology, under a contract with the National Aeronautics and Space Administration.

the critical entry, descent, and landing (EDL) phase of the mission [2]. During the entry, the UHF carrier emitted by Phoenix was received by three orbiting relay spacecraft: NASA's Mars Reconnaissance Orbiter (MRO) and Mars Odyssey (ODY), and the European Space Agency's Mars Express (MEX). The received carrier signals emitted by Phoenix were recorded on the orbiting spacecraft and then relayed via direct-to-Earth (DTE) telemetry to NASA's Deep Space Network tracking stations. The received signal data were analyzed in time and frequency for each link. The time stamps were all synchronized relative to the time of entry at the atmospheric interface[1] (t = 0 s). In addition, the Phoenix UHF carrier was tracked on a DTE link received at the National Radio Astronomy Observatory (NRAO) 100-m-diameter antenna located in Green Bank, West Virginia.

Previous studies of Mars entry blackout suggested that there was a greater potential for a communications blackout during peak heating at the UHF frequency (~401 MHz) used for orbiting relay links [3,4]. Preliminary work on the Phoenix EDL entry to characterize communications at its UHF link frequency of 401.585625 MHz was performed by Gulick[2] and Morabito.[3] Prior to the scheduled EDL event for the Phoenix spacecraft at Mars, preflight predictions of an expected blackout of the radio links suggested a 1 ± 1 min outage period centered around peak heating. The outage period was thus predicted to range from no outage to a maximum of 2 min, assuming conservative uncertainties believed to be the case during early preflight analysis. These bounds were based on most-favorable and worst-case assumptions of the Phoenix entry parameters, and there was no specific orbiter relay link trajectory information available at the time. Atmospheric entry velocities of up to 5.8 km/s were used in the analysis considering several possible trajectories. The predictions were made on the basis of electron number density contour plots about the vehicle generated by aerothermodynamic prediction tools at selected times during entry, when peak heating was expected to occur.

In actuality, Phoenix entered the Martian atmosphere on May 25, 2008, and did not suffer a signal outage (blackout) to any of the three orbiter relay links during the period around peak heating. The preliminary electron number density profile estimates about the vehicle used for the worst-case predictions were based on a higher entry velocity (5.8 km/s) than what was actually flown (5.6 km/s), as it was intended to be conservative. However, during postflight analysis, a close inspection of the received signal data revealed significant fades (brownout) that coincided with high levels of electrons that enveloped the vehicle during the period around peak heating, as predicted by the aerothermodynamic entry analysis.

Aerothermodynamic analyses programs such as NASA Langley's LAURA[4] program [5] can be used to estimate the electron number density profile about a vehicle for atmospheric entry scenarios. By comparing the maximum electron number density that the radio path crosses in a LAURA-output contour plot against the critical electron number density, one can infer whether there is a potential for degradation or blackout. Earlier postflight analysis for Mars Pathfinder and predictions for the Mars Exploration Rovers [4] assumed an "on-off switch"

[1] The atmospheric entry boundary for Mars is defined as a planet-centered spherical shell with a radius of 3522.2 km corresponding to an altitude of 128 km with respect to the mean planetary radius of 3394.2 km.
[2] D. Gulick, "Mars Spacecraft-to-Spacecraft Entry, Descent, and Landing (EDL) Navigation Plasma Analysis for Determining Communications Blackout during Mars Entry," Lockheed-Martin Interoffice Memo WS-06-003 (internal document), Denver, Colorado, July 20, 2006.
[3] D. Morabito, *Phoenix EDL Communications Blackout Analysis* (internal document), Jet Propulsion Laboratory, Pasadena, California, February 9, 2005.
[4] Langley Aero-thermodynamic Upwind Relaxation Algorithm.

approach, "blackout" or "no blackout," based on predictions of traversed electron number density by the signals. A more detailed analysis was employed for Phoenix that involved estimation of the attenuation along the propagation path to the relay orbiters during the period around peak heating at selected times in the trajectory using the electron number density profiles output from LAURA (Section II). The attenuation estimates were compared with the observed attenuations on all three orbiter relay links (Section III). It was found that the estimated attenuation using models agreed with the observed values within the factor-of-10 uncertainty of the LAURA electron number density estimates. This was based on engineering judgment of uncertainty in the LAURA afterbody flowfield predictions given the two-temperature model being used. The LAURA-based attenuation estimates suggested that the model electron number densities were being overestimated by a larger factor early in the brownout period, and approaching closer agreement nearer the end of the brownout period for some links. Possible causes of this overestimation may be that recombination rates of ions to neutrals are higher than currently modeled. This is now a focus of further investigation, as such data may be useful for refining aerothermodynamic models used in LAURA. Thus, the observed fades around peak heating provide supporting evidence that reflection and absorption of signal energy off of the plasma sheath about the vehicle was responsible for these fades, seen on all three orbiter relay links during Phoenix's atmospheric descent. An inspection of detailed spectra at selected times during entry revealed further evidence in the form of broadened carrier energy over frequency as expected for the case of propagation of a narrowband tone through a plasma (Section IV). Finally, we discuss the analysis of the received carrier on the Phoenix-to-NRAO Green Bank DTE link and its suggested association with the orbiting relay link results (Section V).

II. Attenuation Model

In order to predict signal attenuation due to the radio path traversing a cloud of charged particles for a given entry scenario, we make use of theoretical model formulation. We will neglect the presence of a magnetic field in the plasma.

The permittivity of a medium containing charged particles is given by [6]

$$\varepsilon = \varepsilon_0 \left[1 - \frac{Nq^2}{\varepsilon_0 \, m_e (\nu^2 + \omega^2)} - j\left(\frac{\nu}{\omega}\right) \frac{Nq^2}{\varepsilon_0 \, m_e (\nu^2 + \omega^2)} \right] \tag{1}$$

where q is electron charge (1.6×10^{-19} coulombs), ν is the collision frequency of the electrons with neutral atoms, ω is the radio link frequency (rad/s), N is the electron number density (m^{-3}), m_e is electron mass (9.11×10^{-31} kg), and ε_0 is the permittivity of free space (8.85×10^{-12} farad/m^2). From Equation (1), the real and imaginary components of the permittivity can be partitioned such that $\varepsilon = \varepsilon' - j\,\varepsilon''$. The propagation wave number is thus expressed as [6]

$$k = \omega \sqrt{\mu (\varepsilon' - j\,\varepsilon'')} \tag{2}$$

where μ is the magnetic field permeability of free space ($4\pi \times 10^{-7}$ N/Amp^2).

For this analysis, we will neglect the effect of electron collisions on attenuation (thus, $\nu = 0$). The effect of electron collisions on attenuation for other hypersonic vehicle entry cases has been discussed elsewhere in the literature [7,8]. The effect of collisions is expected to be a second-order effect and will be a subject of future study for the Mars Phoenix atmospheric entry case.

The wave number given in Equation (2) for a plasma frequency of $f_p\,(\omega_p/2\pi)$ and link frequency of $f\,(\omega/2\pi)$, (where $f < f_p$), can be shown to be

$$k = \omega\sqrt{\mu\varepsilon_0}\sqrt{\frac{f^2 - f_p^2}{f^2}} \tag{3}$$

where the plasma frequency is related to the electron number density N_e by the following:

$$f_p = \frac{1}{2\pi}\sqrt{\frac{q^2 N_e}{\varepsilon_0 m_e}} \tag{4}$$

and where q, N_e, f_0, and m_e are as defined earlier.

When $f < f_p$, k^2 is negative and we will have pure attenuation of the propagating wave. The attenuated field is expressed in terms of the free space field E_0 and attenuation coefficient $\alpha\,(\alpha = jk)$ as a function of propagation distance z as follows:

$$E(z,t) = E_0 e^{-\alpha z} \tag{5}$$

Thus, the expected attenuation in signal power can be expressed as

$$Att(dB) = 10\,LOG_{10}\left(E(z,t)/E_0\right)^2 = 20\alpha\,LOG_{10}(e) \tag{6}$$

It can be shown from the above formulation (using $\alpha = jk$) that attenuation in dB per unit length through the plasma (z_p) can be expressed thusly:

$$Att(dB/z_p) = \frac{54.6}{\lambda}\sqrt{\frac{f_p^2 - f^2}{f^2}} \tag{7}$$

It would be instructive to calculate electron number density versus time profiles for each signal link by working backwards with input dB attenuation relative to the baseline signal strength (trend in the absence of a plasma). These can then be compared with electron number density profiles at particular time instances inferred from contour plots generated by aerothermodynamic tools along selected aspect angles of the radio link through the path of the plasma enveloping the vehicle. By combining Equations (4) and (7), we can derive an expression for the equivalent electron number density (N_e) in terms of measured attenuation (dB) through a plasma layer of span z_p as follows:

$$N_e = 4\varepsilon_0 m_e\left(\frac{\pi f}{q}\right)^2\left[\frac{\lambda^2(dB/z_p)^2}{54.6^2} + 1\right] \tag{8}$$

In the above formulation, we ignore any complexities associated with introducing a magnetic field. The electron number density is assumed to be a constant through this path, for simplification purposes. In practice, one would need to account for the varying electron number density along the signal path defined by the antenna aspect angle at a given point in time. We can make appropriate use of the above equations and convert to integral form by treating the path variable as a variable of integration.

In general, one can characterize the changing electron number density $N_e(z)$ as a function of the radio path z through the plasma sheath extending from the vehicle surface (z = 0) to some point beyond the plasma cloud ($z = z_p$). A model estimate of the attenuation can be obtained using this profile by performing the following integration and then comparing the estimate against a measurement at a particular point in time:

$$\mathrm{Att\,(dB)} = \int_0^{z_p} \frac{54.6}{\lambda} \sqrt{\frac{q^2 \gamma N_e(z)}{\omega^2 \varepsilon_0 m_e} - 1}\, dz \tag{9}$$

For this analysis, we make use of the correction factor γ, which multiplies the electron number density in Equation (9) (normally unity) in order to match the estimate with the observed attenuation in dB. Thus, Equation (9) represents the model attenuation estimated from an electron number density profile $N_e(z)$ obtained from LAURA. The derived correction factors, γ, evaluated at selected times in the trajectory are discussed in detail later for each orbiting relay link.

As an illustrative exercise, we assume an equivalent electron number density that is constant over a z_p = 50 cm representative scale length: the plasma frequency (f_p) for an electron number density of $3 \times 10^9/cm^3$ is 491.5 MHz. Assuming a link frequency of $f =$ 401 MHz, the attenuation coefficient takes on a value of 5.94. Using the above formulation, we get 51.6 dB/m of attenuation loss per unit length along the signal path through the plasma. Therefore, over a 50-cm path of constant electron number density, a nominal value of 26 dB of attenuation should be observable, assuming adequate SNR.

III. Phoenix Communications Links to Orbiters

The signals emitted by the Phoenix entry vehicle during the atmospheric entry were received by MRO, ODY, and MEX. The cone and clock angles from Phoenix to each of the three orbiters during the first 200 s past entry at the atmospheric interface are displayed in Figures 1 and 2, respectively. Here, the time axis refers to time past atmospheric entry. The definitional meaning of cone angle (θ) about the vehicle axis is displayed graphically in Figure 3.

The wraparound UHF antenna used for communications during the EDL phase, which includes atmospheric entry, is also shown in Figure 3. The wraparound feature ensures a degree of signal reception mostly independent of the clock angle direction of individual orbiting spacecraft. The gain pattern of the UHF wraparound antenna, useful for link characterization and interpretation of received data, is shown in Figure 4.

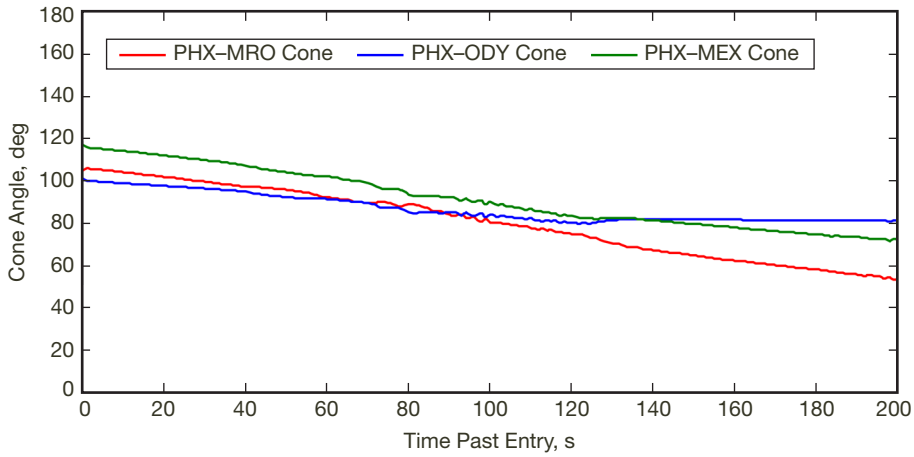

Figure 1. Cone angles for all three orbiter links.

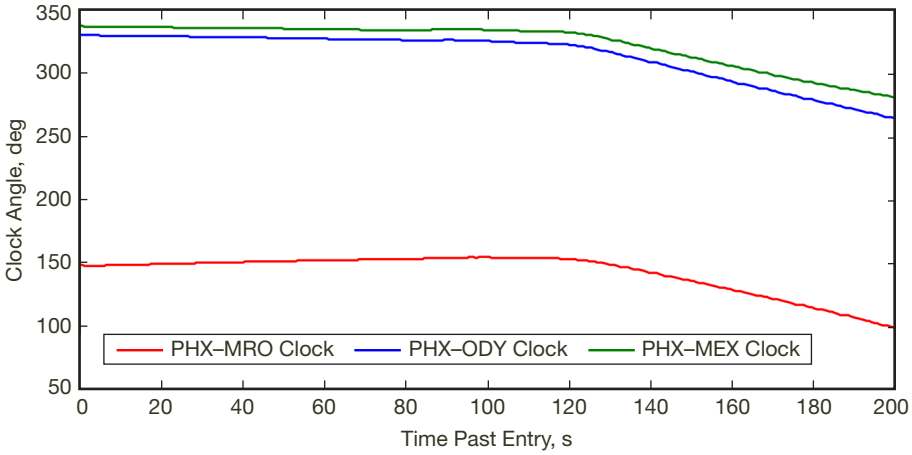

Figure 2. Clock angles for all three orbiter links.

The received signal strength data acquired for all three orbiting spacecraft links were processed and superimposed on Figure 5(a) for comparison purposes. The conditioning of the recorded data sets included processing to extract signal amplitude, applying time stamp corrections to refer to a common time axis, and the removal of a background signal amplitude trend before and just after the expected brownout period such that 0 dB defines the baseline signal level in the absence of degradation due to charged particles.

The MRO signal levels presented in Figure 5(a) were estimated from processing of the in-phase (I) and quadrature (Q) samples of the carrier that were recorded onboard MRO at a 150-kHz rate and telemetered to Earth on the 8.4-GHz (X-band) DTE link. The processing of the samples involved performing fast Fourier transforms (FFTs) at 1-Hz bin resolution. The output signal level power measurements involved an integration of the energy within ±17 bins centered on the bin with peak signal power for each FFT. The relative signal power was then output for each 1-s time period. The time series over the entire EDL period was first examined and it was found that there was a period of fading coinciding with the

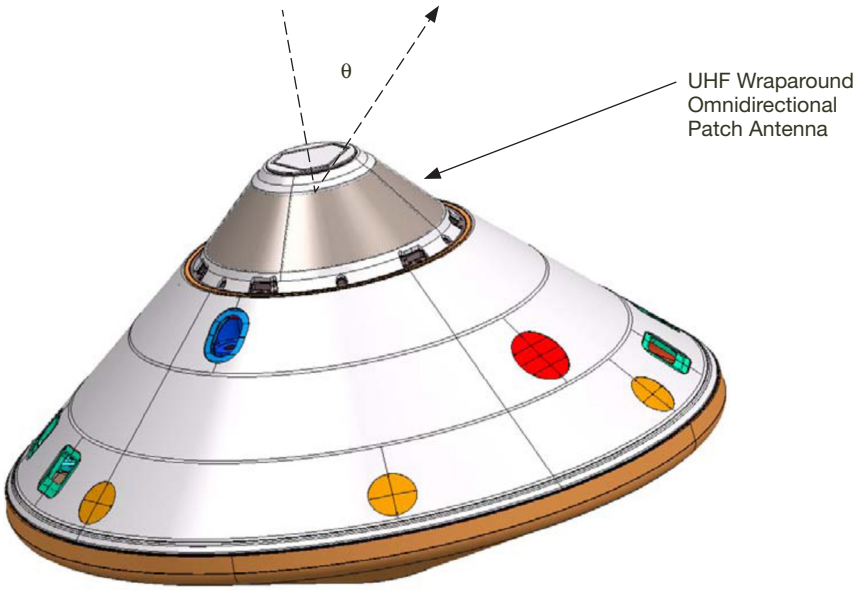

Figure 3. Diagram depicting backshell and heatshield layout of Phoenix aeroshell used during atmospheric entry.[5] Also shown is the definition of cone angle, θ, between the spacecraft axis and direction of orbiting relay asset (dashed arrow).

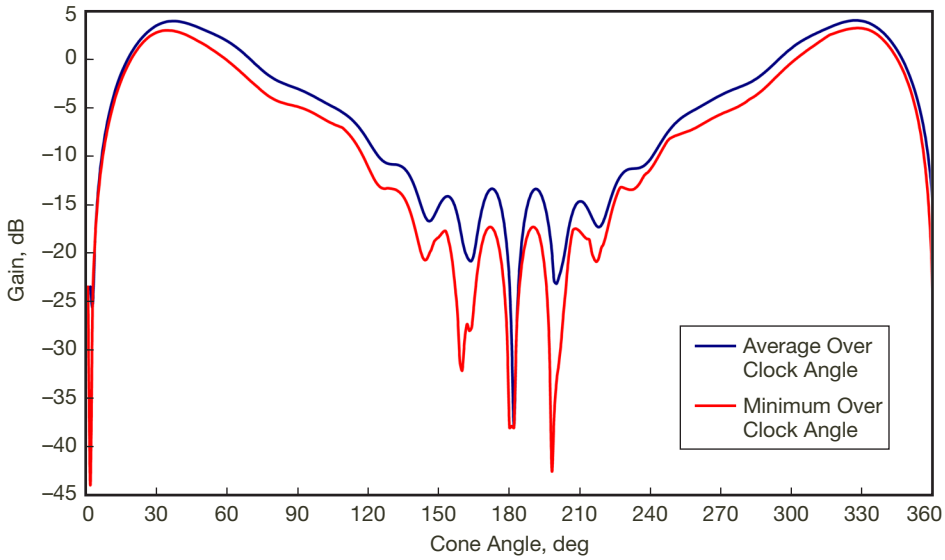

Figure 4. Phoenix UHF wraparound antenna pattern.[6]

predicted brownout period. A selected subset of points on each side of the brownout period was averaged to yield two baseline points establishing an undisturbed background trend. A straight line fit to these two points was then removed from the data series. The resulting time series for the brownout period is shown in Figure 5(a) for MRO such that 0 dB establishes the background level. Similar processing techniques were applied for the Phoenix-to-Odyssey and Phoenix-to-MEX data sets.

[5] D. Lee, *Phoenix Telecom Design Control Document*, JPL D-12345 (internal document), Jet Propulsion Laboratory, Pasadena, California, June 9, 2006.
[6] Ibid.

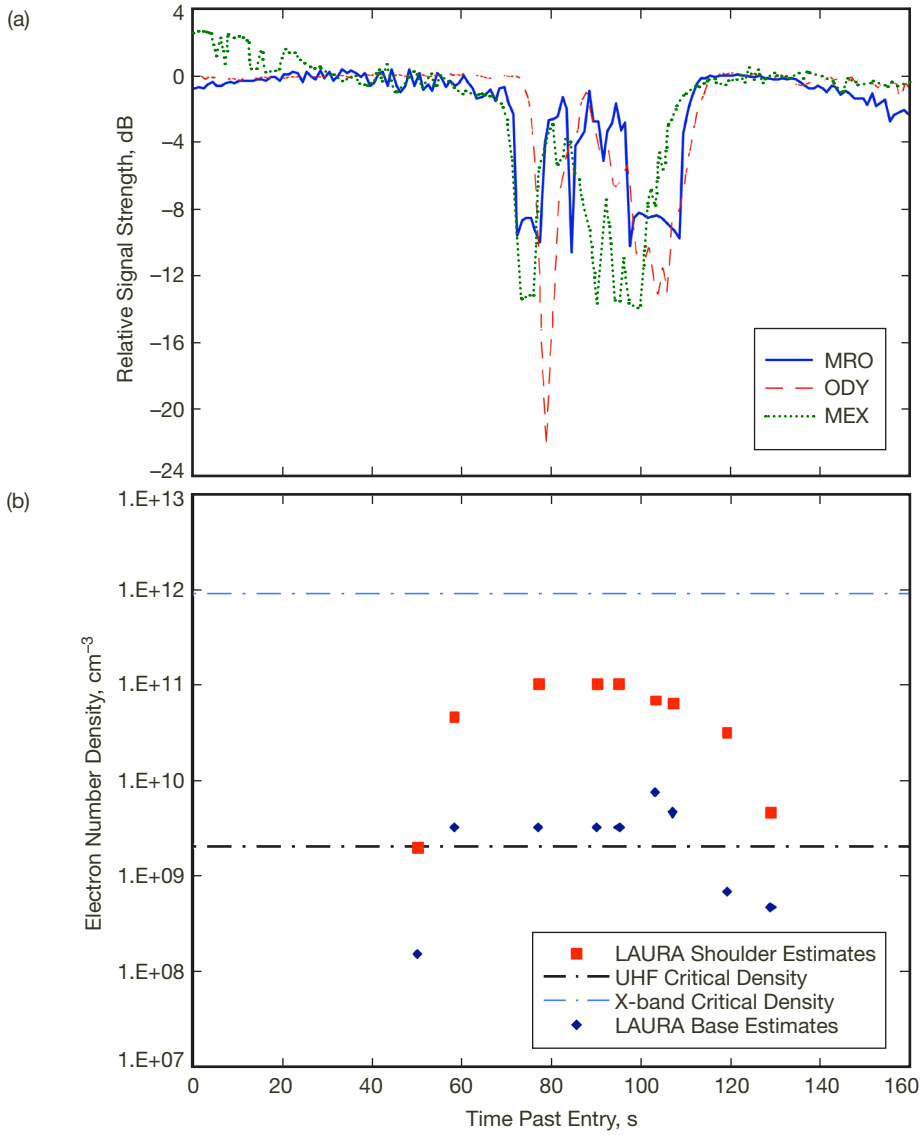

Figure 5. (a) Relative signal strength time series showing degradation versus time past atmospheric entry for all three Phoenix-to-orbiter links. Signal strength measurements have been corrected by removing a background trend just before and just after the degradation period. (b) Phoenix EDL plasma number density extracted from preflight LAURA runs.[7,8] Red points depict maximum values through shoulder direction (θ = 90 deg) and blue points depict maximum values through base (θ = 0 deg). Also shown are critical number density profiles (see legend).

The resulting fade signatures for all three orbiter links clearly coincide with each other within the same time period [Figure 5(a)]. Such behavior cannot be explained by phenomena such as variations with antenna aspect angle or dynamics (Doppler spreading). For instance, during the period of signal degradation, the cone angle of the MRO radio link about Phoenix changed from 90 deg at 71 s to 78 deg at 113 s past entry. Based on an examination of the wraparound patch antenna pattern in Figure 4, the radio path was obviously well within the main continuous portion of the pattern, and thus such signal variations could

[7] D. Gulick, op. cit.
[8] D. Morabito, op. cit.

not be explained by going in and out of nulls. The Doppler rate during and just outside the brownout period was reasonably constant, near 36 Hz/s. Thus, the FFT algorithm making use of integrating signal energy over ±17 Hz worth of bins allowed for reasonable estimation of signal power smeared over frequency during this period. The observed fades thus could not be caused by Doppler spreading, which was of consistent character inside and outside the brownout period.

When the time series of these signal variations [Figure 5(a)] is compared against a preflight time series of electron number densities [Figure 5(b], it is clearly seen that the signal fades coincide with the period of elevated peak electron number densities exceeding the critical value for UHF brownout/blackout, either looking out of the shoulder (red) or base (blue) direction about the vehicle. Thus, this provides strong evidence that the signal level reductions are likely due to brownout resulting from enhanced levels of charged particles near the vehicle that crossed the signal paths.

Detailed analysis of the received carrier data for each orbiter link reveals that during the strongest fades (or weakest signal levels), the Phoenix-to-orbiter received signal power levels still exceeded the noise floor. The Phoenix orbiter links thus had sufficient SNR to overcome blackout, and the reduced signal levels during the period around peak heating are likely due to brownout caused by enhanced levels of charged particles. The measured attenuations for selected time instances during entry (listed in Table 1) will be compared with estimates derived from LAURA electron number density profiles using Equation (9) along the applicable cone angles.

The preflight predictions of electron number density provided in Figure 5(b) were generated for a more conservative trajectory than what was actually flown. The LAURA aerothermodynamic program was rerun using parameters based on a more representative trajectory for the selected time instances displayed in Table 1 (column 1), and these results will be presented here. Table 1 also displays the clock and cone angles about the vehicle to each orbiter relay link at the selected time instances.

Table 1. Phoenix to orbiter: clock and cone angles for selected times.

Time Past Entry, s	PHX–MRO Clock, deg	PHX–MRO Cone, deg	PHX–ODY Clock, deg	PHX–ODY Cone, deg	PHX–MEX Clock, deg	PHX–MEX Cone, deg
68	152.5	90.1	326.6	90.2	334.2	99.8
75	152.9	89.6	326.2	87.4	334.1	96.2
79	153.0	88.6	326.0	86.5	333.9	94.9
88	153.9	85.7	326.0	85.0	334.2	92.3
92	154.3	84.1	326.0	84.6	334.4	91.4
103	154.0	79.8	324.8	83.5	333.7	89.0
108	153.9	78.6	324.1	82.4	333.2	87.1

A. Communications Link: Phoenix to Mars Reconnaissance Orbiter (PHX–MRO)

During the entry phase, MRO was configured for open-loop record mode where carrier and 8-kbps telemetry spectra were captured. Phoenix transmitted 8-kbps telemetry in unreliable bitstream mode [2]. The received power recorded on MRO during the period around atmospheric entry and extracted from spectral processing is shown in the blue curve of Figure 5(a). The baseline signal strength just before and after the fade period was used to remove the background trend (such as due to changing antenna pattern gain with aspect angle) to set the baseline attenuation to zero — 0 dB on the Figure 5(a) vertical axis.

The signal fades span the times from roughly 60 s to 110 s past entry, coinciding with the predicted blackout/brownout period. The signal level during the weakest fades lies above threshold for a given signal processing scheme. This is based upon an examination of FFT snapshots showing that the carrier is still present with adequate SNR. Thus, we assume that the weakest signal levels of the fades are representative of attenuation measurements and not noise floor.

The relative signal strength of the Phoenix UHF carrier received at MRO versus time past atmospheric entry is shown in Figure 5(a) for the time interval of interest occurring near peak heating. Figure 5(b) presents electron number density profiles for both shoulder (θ = 90 deg) and base (θ = 0 deg) directions using a conservative case trajectory with a 5.8 km/s entry velocity.[9] The wake region (shoulder and base) electron number density profile is shown in Figure 5(b) to traverse just above the critical electron number density threshold at the 401-MHz link frequency between 57 s to about 110 s past entry. Not coincidentally, one can see that the period of signal degradation falls within this same time period. The level of signal degradation ranges to about 10 dB or more with some periods showing partial recovery of the signal. The complex nature of the variations seen in Figure 5(a) may be due to a combination of the signal path traversing different regions of electron number density as the antenna aspect angle changes, changes in electron number density itself due to turbulence about the vehicle, as well as possibly a small amount of unmodeled response of the activated automatic gain control (AGC) circuitry in the MRO Electra radio to received signal level changes. There may also be cases where the plasma sheath may act to reflect some signal energy back towards the receiver due to favorable geometry of the sheath with respect to the radio path.

Figure 6 illustrates an example LAURA contour plot based on the best available trajectory solution at 103 s past entry. An interesting feature can be seen between 100 to 112 s past entry [Figure 5(a) blue curve], where the degradation ranged from about 8 to 10 dB. Upon examining Figure 6, one can see that the signal path to MRO intersects values of electron number density that exceed the $2 \times 10^9/\text{cm}^3$ critical electron number density for the UHF link frequency. Upon further examination, the observed signal level degradation has been seen to coincide with elevated levels of electron number density that lie above the UHF threshold during several selected time instances during this period at the expected signal link directions.

[9] D. Morabito, op. cit.

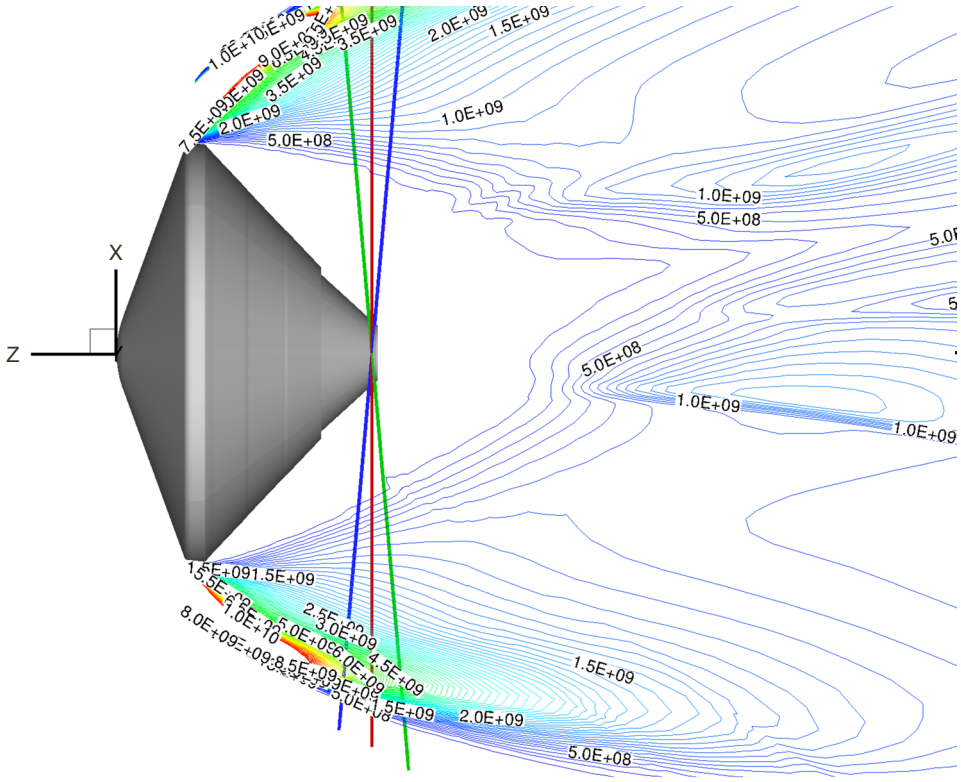

Figure 6. Mars Phoenix, reconstructed trajectory (t = 103 s, angle of attack = 2.52 deg). LAURA electron number density contours (cm^{-3}) about the vehicle at 103 s past atmospheric entry with selected cone angle slices (solid straight lines) for wind-side and lee-side, corresponding to directions at 85 deg, 90 deg, and 95 deg from the edge of the wraparound UHF antenna. The directions to all three orbiting spacecraft lie within this range of angles. The y-axis points down perpendicular to the page.

As shown in the LAURA plots, the plasma density changes as a function of distance along the radio line of sight, and thus a complex scheme was employed to estimate model attenuation. This approach makes use of Equation (9) in Section II using an integration of the electron number density profile from LAURA along the known antenna aspect angle (cone angle) at each select time instance such as listed in Table 1. The results of this approach are discussed in Section III.D.

B. Communications Link: Phoenix to Mars Odyssey (PHX–ODY)

During atmospheric entry, Mars Odyssey (ODY) was configured in canister mode where only carrier and Doppler information could be extracted from recorded spectra [2]. The received carrier power time stamps were corrected to reference time relative to atmospheric entry. A background signal level trend before and after the period around peak heating was removed to produce attenuation measurements. The received relative carrier power from Odyssey is displayed in Figure 5(a), red dashed curve, where the variations between 70 s and 110 s again coincide with the anticipated blackout/brownout period. Here, the weakest signal level was well above the –134 dBm modulated carrier threshold for the PHX–ODY link [2]. Thus, we reemphasize the correlation of signal degradation [Figure 5(a) red curve] against the electron number density peak profile around peak heating [see Figure 5(b)]. The

largest and sharpest fade occurs near 79 s past entry for the PHX–ODY link, a fade level of about 22 dB. The signal then builds back up to near-baseline levels at 88 s past entry, degrades again down near peak heating at 104 s, and then recovers to baseline levels near 119 s. LAURA contour plots of electron number density for 75 s and 79 s occurring near the time of the large 22 dB fade do show significant plasma density levels along the expected signal paths that exceed the critical level for UHF.

Figure 7 illustrates an example of a LAURA contour plot at 75 s past entry. Figure 8 displays the corresponding electron number density profiles versus the distance from the vehicle in the directions of 85-deg, 90-deg and 95-deg cone angles where the three orbiting spacecraft were located at 75 s, as extracted from the data of Figure 7. The wind-side (negative x) electron number densities are generally larger than the lee-side (positive x) values because the shock layer is stronger on that side due to the orientation of the velocity vector relative to the vehicle axis. Figure 9 displays the electron number density profile information in the directions of 85-deg, 90-deg, and 95-deg cone angles at 103 s past entry.

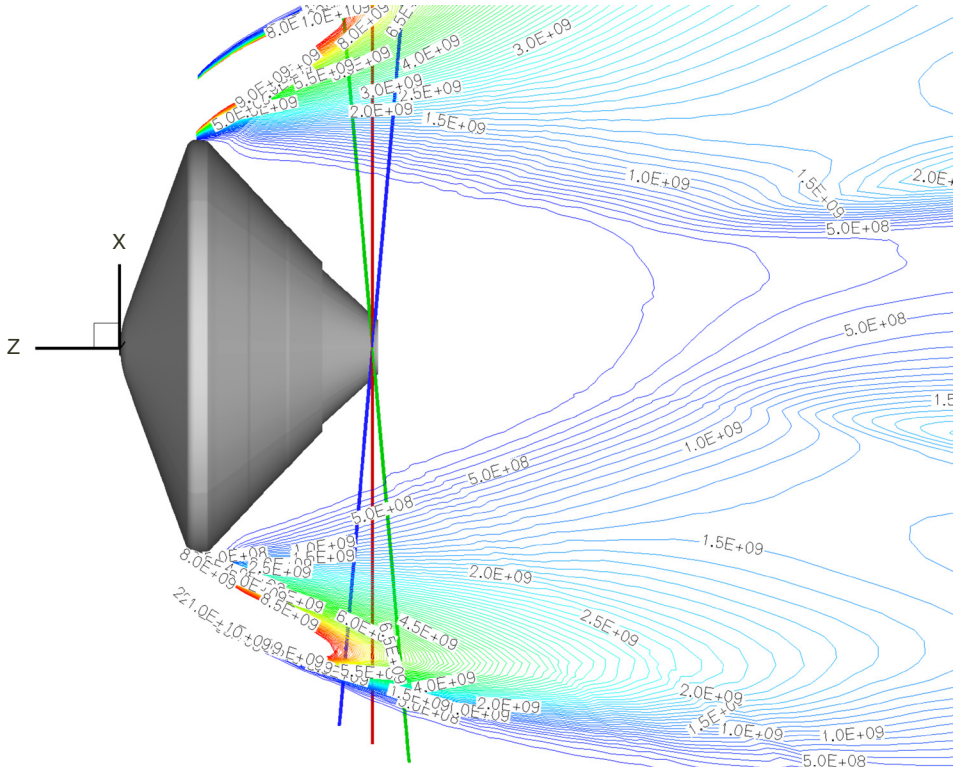

Figure 7. Mars Phoenix, reconstructed trajectory (t = 75 s, angle of attack = 1.97 deg). LAURA electron number density contour plot (cm^{-3}) about Phoenix at 75 s past entry showing selected cone angle slices (solid straight lines) through the plasma sheath for both wind-side and lee-side, corresponding to 85 deg, 90 deg and 95 deg from the edge of the wraparound UHF antenna. The y-axis points down perpendicular to the page.

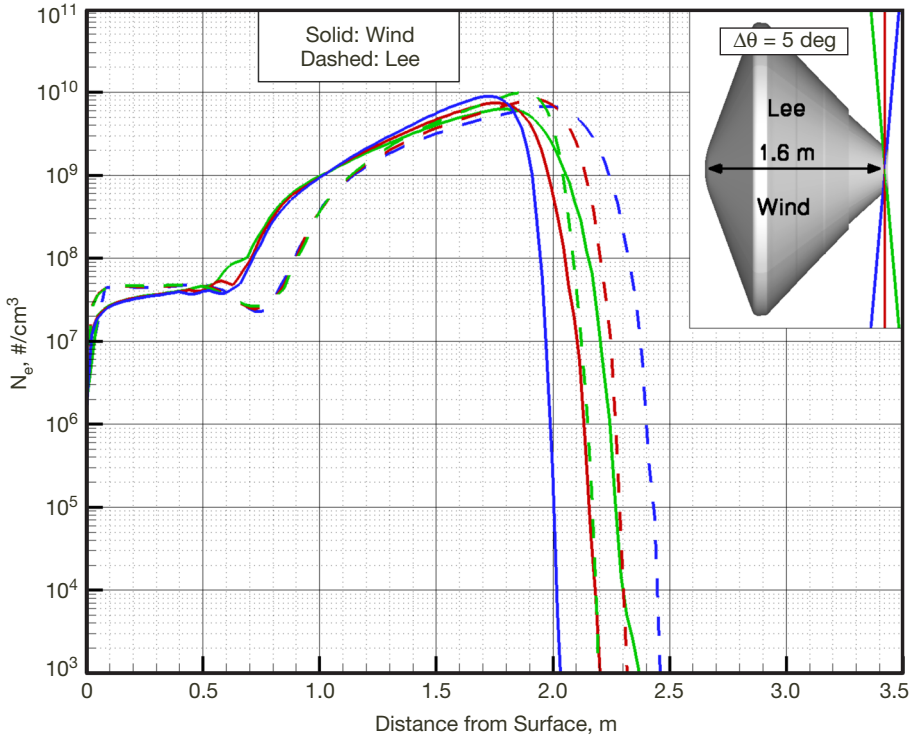

Figure 8. Mars Phoenix, reconstructed trajectory (t = 75 s, angle of attack = 1.97 deg). Electron number density profile along selected cone angle cuts for 75 s past entry time instance.

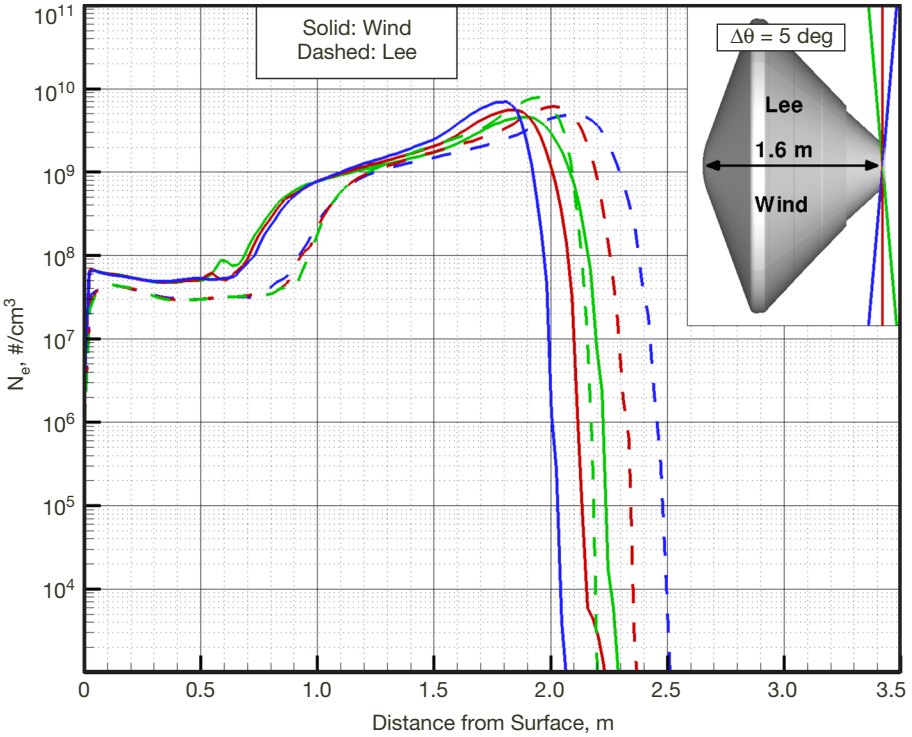

Figure 9. Mars Phoenix, reconstructed trajectory (t = 103 s, angle of attack = 2.52 deg). Electron number density profile along selected cone angle cuts for 103 s past entry time instance.

As seen from the cone angle signature (Figure 1), this angle of the PHX–ODY signal ray path ranges from 82 deg to 91 deg during the signal fade period seen in Figure 5(a), red dashed curve. The signal strength of the fade at 79 s past entry at its weakest point appears to have about 6 dB SNR according to a check of carrier spectra at this time, suggesting that the entire fade event is representative of measured attenuation and does not include the noise floor. Thus, the entire time series of signal strength measurements during the brownout period can be assumed to be attenuation measurements that can be correlated against model predictions estimated from electron number density profiles output from LAURA. Another large fade event for the PHX–ODY link is seen near 104 s in Figure 5(a), red dashed curve, with an 83-deg aspect angle. The LAURA contour plot at 103 s shows significant electron density exceeding the critical level.

C. Communications from Phoenix to Mars Express (PHX–MEX)

The relative signal strength plot for the Phoenix-to-Mars Express link is shown in Figure 5(a), green dotted curve. Here, we see some similarity with the PHX–MRO signature [see Figure 5(a), blue curve] with a 12-dB fade near 70 s and some fading near 12-dB levels between 90 and 100 s. A close examination of the spectral data at the times of the deepest fades suggests that there is still adequate SNR in the received carrier signal to allow its detection, so that we can be confident that the weakest point of fade signatures for PHX–MEX are measurements of signal attenuation and not the result of reaching the noise floor. Again, the measured attenuation time series, this time for PHX–MEX in Figure 5(a), green dotted curve, falls clearly within the period of increased electron number density [Figure 5b)], exceeding the critical threshold for signal degradation during Phoenix atmospheric entry. During the signal degradation period, the PHX–MEX cone angle changed from 99 deg near 69 s past entry to 87 deg near 110 s past entry.

D. Integrated Analysis of the Three Phoenix-to-Orbiter Links

An initial cut on integrating the electron number density along the raypaths toward the orbiters to extract predicted attenuation using Equation (9) was conducted for the cases corresponding to the time instances provided in Table 1. It was found that this estimated attenuation from the integration of electron number density along the radio paths significantly surpassed the observed values when assuming $\gamma = 1$ in Equation (9). It was then decided to adjust γ in Equation (9) to allow the model attenuation to match the measured attenuation. An interesting result was attained if the electron number density profiles along the signal paths of the cone angle cuts were reduced by a constant reduction factor at each epoch. This resulted in the predicted attenuation nicely matching the observed attenuation for all three orbiter links. It is believed that the uncertainty on the LAURA-derived electron number density profiles can be in error by as much as an order of magnitude, which would result in correction factors of γ between 10 and 0.1. The observed correction factors, ranging from 0.218 to 0.890, lie near and mostly well within this error bound. Possible refinements of the models or explanation of the dominating error sources are currently being explored and are a focus of further study.

Table 2 summarizes the correction factors used to match model and observed attenuation for all time instances listed on all three orbiter links. Figure 10 graphically summarizes these correction factors over time for all three orbiter links, and for both wind-side and lee-side directions. The results show that there is not a significant difference between wind-side and lee-side correction factors, thus allowing us to neglect clock angle direction considerations. For times past entry of less than 90 s, the correction factors shown in Figure 10 are all consistent with LAURA overestimating the electron number density profile by roughly a factor of $(1/\gamma) \sim 3)$ — except near 79 s, where there is a large difference between PHX–ODY (~0.5) and PHX–MEX links (~0.22). The larger correction factor for ODY at 79 s is not fully understood since its trajectory location lies near MEX, while MRO is at a clock angle in the opposite direction. However, it is conjectured that the large difference in the PHX–ODY link correction factor at 79 s relative to the other two orbiter links may be related to estimation error at the large 22-db fade value for this link. At peak heating, one expects a wider dispersion of electron number density about the vehicle relative to the LAURA estimates. Above 100 s in Figure 10, the correction factors begin to increase in the direction of improved agreement between measurement and model for electron number density profile (within a factor of 2 for all three links). Here, there is a discernible difference between the PHX–MEX link (which has a cone angle near 90 deg) and the other two orbiter links (whose cone angles lie nearer 80 deg).

Table 2. Plasma attenuation correction factors (γ).

Time Past Entry, s	PHX–MRO Lee-Side	PHX–MRO Wind-Side	PHX–ODY Lee-Side	PHX–ODY Wind-Side	PHX–MEX Lee-Side	PHX–MEX Wind-Side
68	0.332	0.329	0.319	0.318	0.280	0.290
75	0.340	0.365	0.325	0.350	0.320	0.350
79	0.286	0.309	0.495	0.530	0.218	0.246
88	0.322	0.353	0.312	0.340	0.303	0.343
92	0.326	0.359	0.317	0.351	0.289	0.333
103	0.647	0.676	0.615	0.675	0.457	0.495
108	0.830	0.890	0.750	0.810	0.500	0.550

There is a consistent trend between larger cone angles and higher levels of measured attenuation. For instance, at 75 s past entry, ODY data show a 3-dB fade at 85-deg cone angle, which is looking through less plasma than the MRO link with 10 dB of attenuation at 90 deg. The MEX link shows an even higher level of attenuation of 13 dB at 95-deg cone angle.

At 103 s past entry, we see that both the PHX–MRO and PHX–ODY links display consistent behavior corresponding to a correction factor of about $\gamma \sim 0.65$ (Table 2 and Figure 10) through the LAURA plasma paths at their respective cone angles. The MEX link result seems to imply a lower amount of plasma by almost 1/2, but the 103-s sampled point is on a large upslope portion of the MEX fade as it is recovering and the cone angle is near 90 deg where

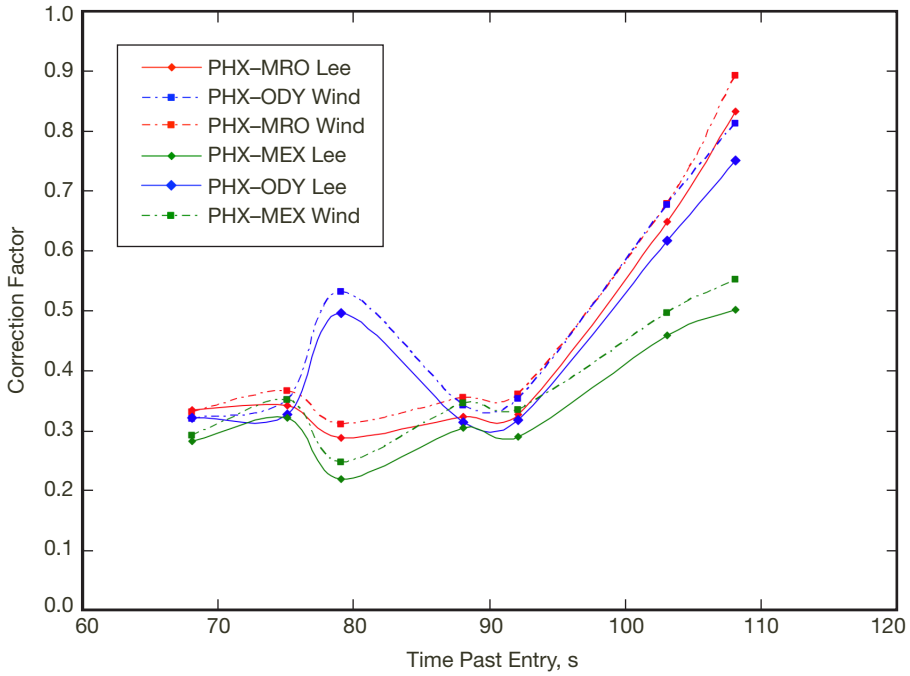

Figure 10. Correction factors (γ in Equation 9) used to match measured and integrated model attenuation for each Phoenix orbiter link for both lee-side and wind-side density profiles. The inserted lines are smoothed about the connected data points.

there is likely more plasma turbulence. These differences are consistent with uncertainties in the model and possibly caused by unforeseen temporal variations in the plasma dynamics (turbulence) along the 90-deg cut.

At 108 s past entry in Figure 5(a), we see that large ~9 dB fade strengths are evident for the PHX–MRO and PHX–ODY links with correction factors ranging from γ ~ 0.75 to 0.89, suggesting much better accuracy of the LAURA solutions for these links, whereas the MEX link correction factors of γ ~ 0.5 to 0.55 for the 1.5 dB fade are suggestive of factor-of-2 accuracy in LAURA estimation of the electron number density profiles, still well within the factor-of-10 overall accuracy for the after body density estimates.

Additional LAURA runs at 68 s and 88 s past entry were analyzed for all three orbiter links. For these runs, we found that the resultant correction factors for both lee-side and wind-side electron number density profiles were all close to γ ~ 1/3, within the expected factor of uncertainty in the LAURA estimates, providing a high degree of consistency. This is encouraging since there is a wide range of attenuation for the three orbiter links. At 68 s past entry, there is a small amount of attenuation (~1 dB) measured over all three links [Figure 5(a)]. This is where the onset of the brownout occurs and results in a correction factor that is reasonably consistent with those estimated during higher levels of attenuation later during the heart of the brownout. The consistency of the correction factors for the 88-s past entry results for all three orbiter links provides another confidence check where attenuations ranged from 1 dB for PHX–ODY to 8.8 dB for PHX–MEX.

It was therefore found that there were no significant order of magnitude differences in the plasma attenuation correction factors produced as a result of the fades. Had the estimates of the LAURA electron densities for this trajectory been perfect — i.e., if γ in Equation (9) were unity — then the resulting attenuation would have been extremely large, resulting in total signal blackouts during much of the fade period as the available SNR in each case would have easily been overwhelmed. On the other hand, if the correction factors had been closer to $\gamma \sim 0.1$, an analysis using Equation (9) suggests that there would not have been any appreciable fading observed during the atmospheric entry contrary to the results displayed in Figure 5(a). Thus, we believe the results of Table 2 and Figure 10 are representative of conditions during the Phoenix Mars atmospheric entry.

The trend in the Figure 10 attenuation factors implies an overestimation of electron number density by as much as a factor of 3 during much of the early fade period (at 68 s to 92 s after entry), with better agreement later (103 s and 108 s past entry). This trend appears to be consistent with the use of the two-temperature model used in LAURA. The model assumes that the vibrational and electronic energies of all species, including electrons, are at equilibrium at the same temperature, and that the translational and rotational energies of all chemical species are in equilibrium at another temperature. Early in the fade period, the tying of the electron temperature with the vibrational temperature may not be strictly valid and is likely leading to an overestimation of electron temperature and thus an overestimate of density of free electrons.[10] Later during the period around peak heating, there is improved agreement where the assumption has more validity as LAURA is overestimating the electron number density by only within a factor of 2 of the density necessary to produce the observed fades. An earlier work comparing numerical simulation with experimental data from an Earth flight experiment suggests a similar conclusion [9]. The time of peak heating is estimated to be at 116 s past entry [10], which coincides with the end of the brownout period on all three orbiting relay links. An additional LAURA contour plot generated for this time still shows significant levels of plasma near the shoulder regions about the entry vehicle. However, given that the cone angles for all three links have continued to decrease to smaller values, the resulting ray paths were seen to traverse insufficient plasma to cause any appreciable fading, consistent with the observations. Measurements such as these may be useful in future refinement or calibration of aerothermodynamic models and code. Thus, an examination of the effects of model considerations for aerothermodynamic software (such as the use of different temperature models) and the effects of collisions in attenuation estimates (Section II) are focuses of future work.

IV. Analysis of Carrier Spectra during Fade Periods

The PHX–MRO open-loop receiver carrier data were processed with a third-order phase-locked loop in order to remove uncompensated dynamic effects in the measured attenuation data (smearing of carrier power across multiple frequency bins). These PHX–MRO carrier spectra were produced over a display range from –200 to 200 Hz with a frequency resolution of 1 Hz/bin in order to discern any evidence of broadening in frequency space due to high densities of charged particles. A narrowband signal tone traversing a dense region of charged particles in turbulent motion will experience reflection and absorption of

[10] Peter Gnoffo, personal communication, NASA Langley Research Center, Hampton, Virginia, November 16, 2009.

signal energy off of the plasma. The signal energy output from this plasma will also consist of multiple components spread in frequency space with different levels of Doppler shifts usually centered about the frequency of the undisturbed carrier.

Carrier spectra were generated for each second from the PHX–MRO signal link data during the period covering atmospheric entry. The spectra taken at the various times are well correlated with what is observed, that is, varying levels of broadening of carrier signal power is evident during fade periods. Examples of spectra for two selected times in the PHX–MRO amplitude fade time series of Figure 5(a) are shown in Figure 11. The spectra taken during a very deep fade feature at 84 s past entry is shown in Figure 11(a), Here, we see spreading of the carrier signal covering a range of about 100 Hz (roughly –50 to 50 Hz). For comparison, the uncorrupted carrier at 119 s past entry outside of the brownout period is shown in Figure 11(b).

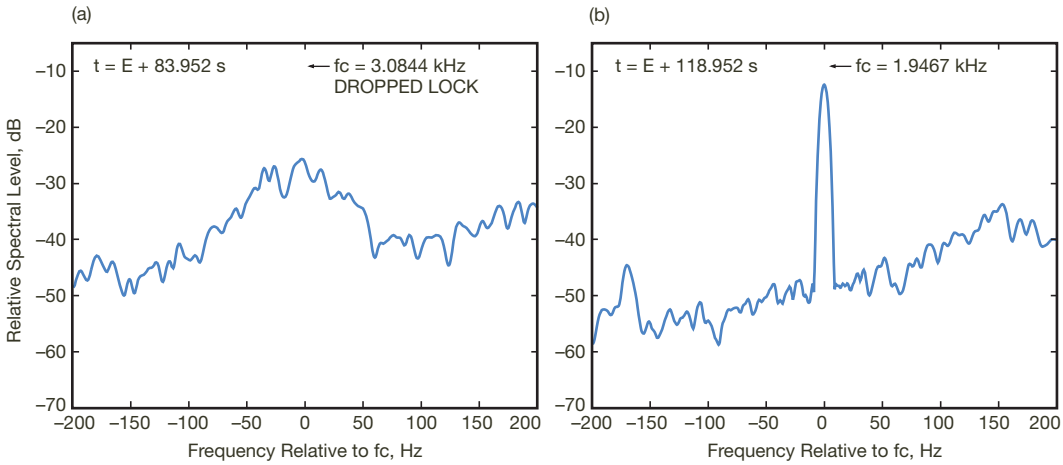

Figure 11. PHX–MRO carrier power spectra (a) during deep fade within plasma-degraded period at 84 s past entry and (b) during undisturbed period outside of brownout at 119 s past entry.

Several of the broadened spectral plots generated during the fade periods show asymmetries as expected, as signal energy may be reflected or diffracted off of varying density structures in different ways about the vehicle. The presence of significant broadening of the carrier during the period of peak heating provides additional evidence that the observed brownouts (fades) are indeed attributable to charged particles generated by frictional heating during atmospheric entry. Evaluation of a refined Doppler compensation scheme for the open-loop carrier data is the focus of future work along with performing the Doppler compensation processing on the other Phoenix-to-orbiter links.

V. Analysis of Received Carrier at Green Bank

The carrier emitted by Phoenix was also observed on a DTE link using the UHF-equipped receivers at the large NRAO 100-m-diameter antenna in Green Bank, West Virginia. A radio science open-loop receiver was operated in a predict-driven mode compensating for Doppler; thus, dynamic activity was not expected to degrade the link. According to preflight link analysis, the expected SNR of this link during the period around peak heating was very

weak at or near the threshold level (1 to 2 dB). An outage in the signal strength data was observed during the predicted blackout period (between roughly 64 s to 120 s) discussed in this article. This can be attributed to the very low SNR of the received signal at Green Bank being degraded using the knowledge of the expected attenuation levels that we measured and predicted for the three orbiting spacecraft links discussed in this article. The detailed analysis of the Phoenix-to-Green Bank carrier data is a focus of future study.

VI. Conclusion

Phoenix entered the Martian atmosphere on May 25, 2008, and did not suffer a signal outage (blackout) to any of the three orbiter relay links during the period near peak heating. However, a close inspection of the received signal data for the three orbiting spacecraft links with Phoenix revealed significant fades (brownout) that coincided with high levels of electrons that enveloped the vehicle during the period around peak heating, as predicted by the aerothermodynamic entry analysis. A detailed analysis was employed for the Phoenix orbiter links that involved estimation of the attenuation along the vehicle cone angles to the relay orbiters during the period near peak heating at selected times in the trajectory using the electron number density profiles output from LAURA. The LAURA-based attenuation estimates were compared with the measured attenuations on all three orbiter relay links. It was found that the model estimates usually agreed with the observations within the expected factor-of-10 uncertainty of the LAURA electron number density estimates in the afterbody region. The LAURA program appears to be overestimating electron number density well within its factor-of-10 uncertainty limit for most cases analyzed. Analysis of carrier spectra revealed carrier broadening correlated in time with observed signal fades, providing additional evidence that signal degradation is attributable to charged particles about the vehicle caused by the frictional heating of atmospheric gases as Phoenix entered the Martian atmosphere. Such modeling techniques can be applied to future EDL scenarios such as that for the upcoming Mars Science Laboratory (MSL) mission. In addition, such information extracted from the observations can be used to refine modeling in aerothermodynamic software.

Acknowledgments

We appreciate the support of Chad Edwards of the Mars Program Office at the Jet Propulsion Laboratory in funding and reviewing this work. We would also like to thank Peter Ilott and Prasun Desai for many informative discussions pertaining to this study. We also appreciate the open-loop data provided for inspection by the Radio Science Support Team at JPL (Sami Asmar, Danny Kahan, Sue Finley, and Aseel Anabtawi).

References

[1] D. E. Mather, J. M. Pasqual, J. P. Sillence, and P. Lewis, “Radio Frequency (RF) Blackout during Hypersonic Reentry,” AIAA 2005-3443, AIAA/CIRA 13th International Space Planes and Hypersonics Systems and Technologies Conference, Capua, Italy, May 16–20, 2005.

[2] R. P. Kornfeld, M. D. Garcia, L. E. Craig, S. Butman, and G. M. Signori, "Entry, Descent, and Landing Communications for the 2007 Phoenix Mars Lander," *Journal of Spacecraft and Rockets*, vol. 45, no. 3, pp. 534–547, 2008.

[3] D. D. Morabito and K. T. Edquist, "Communications Blackout Predictions for Atmospheric Entry of Mars Science Laboratory," *2005 IEEE Aerospace Conference Proceedings*, IEEE Publications, Piscataway, N. J., pp. 489–500, March 5–12, 2005.

[4] D. D. Morabito, "The Spacecraft Communications Blackout Problem Encountered during Passage or Entry of Planetary Atmospheres," *The Interplanetary Network Progress Report*, vol. 42-150, Jet Propulsion Laboratory, Pasadena, California, pp. 1–23, August 15, 2002. http://ipnpr.jpl.nasa.gov/progress_report/42-150/150C.pdf

[5] P. A. Gnoffo, R. N. Gupta, and J. L. Shinn, *Conservation Equations and Physical Models for Hypersonic Air Flows in Thermal and Chemical Non-Equilibrium*, NASA Technical Paper 2867, National Aeronautics and Space Administration, Hampton, Virginia, 1989.

[6] S. Ramo, J. R. Whinnery, and T. Van Duzer, *Fields and Waves in Communications Electronics*, John Wiley and Sons, Inc., New York, 1967.

[7] R. A. Hartunian, G. E. Stewart, S. D. Fergason, T. J. Curtiss, and R. W. Seibold, *Causes and Mitigation of Radio Frequency (RF) Blackout during Reentry of Reusable Launch Vehicles*, Aerospace Report No. ATR-2007(5309)-1, The Aerospace Corporation, El Segundo, California, January 26, 2007.

[8] R. Lehnert and B. Rosenbaum, *Plasma Effects on Apollo Re-entry Communication*, NASA Technical Note D-2732, National Aeronautics and Space Administration, Washington, D.C., March 1965.

[9] P. A. Gnoffo, "Code Calibration Program in Support of the Aeroassist Flight Experiment," *Journal of Spacecraft and Rockets*, vol. 27, no. 2, pp. 131–142, March–April 1990.

[10] P. N. Desai, J. L. Prince, E. M. Queen, and M. R. Grover, "Entry, Descent, and Landing Performance of the Mars Phoenix Lander," AIAA Paper 2008-7346, *Proceedings of AIAA Guidance, Navigation, and Control Conference*, Honolulu, Hawai'i, August 2008.